Unidirectional Spin-Wave-Propagation-Induced Seebeck Voltage in a PEDOT:PSS/YIG Bilayer

P. Wang, L. F. Zhou, S. W. Jiang, Z. Z. Luan, D. J. Shu,* H. F. Ding,† and D. Wu‡
National Laboratory of Solid State Microstructures,
Department of Physics and Collaborative Innovation Center of Advanced Microstructures,
Nanjing University, 22 Hankou Road, Nanjing 210093, People's Republic of China

(Received 2 November 2017; published 24 January 2018)

We clarify the physical origin of the dc voltage generation in a bilayer of a conducting polymer film and a micrometer-thick magnetic insulator $Y_3Fe_5O_{12}$ (YIG) film under ferromagnetic resonance and/or spin wave excitation conditions. The previous attributed mechanism, the inverse spin Hall effect in the polymer [Nat. Mater. **12**, 622 (2013)], is excluded by two control experiments. We find an in-plane temperature gradient in YIG which has the same angular dependence with the generated voltage. Both vanish when the YIG thickness is reduced to a few nanometers. Thus, we argue that the dc voltage is governed by the Seebeck effect in the polymer, where the temperature gradient is created by the nonreciprocal magnetostatic surface spin wave propagation in YIG.

DOI: 10.1103/PhysRevLett.120.047201

Interconversion between spin and charge current is one of the most important ingredients in spintronics [1,2]. There are two different types of spin current that transport spin angular momentum: spin-polarized current and pure spin current [3,4]. For the spin-polarized current, which is an electrical charge current with imbalance spins, it can be generated and converted by magnetic conductors [5]. For the pure spin current, which carries angular momentum without an electrical charge current, the spin-charge interconversion is recently known to be realized by the spin Hall effect (SHE) and its reciprocal effect, the inverse spin Hall effect (ISHE), in nonmagnetic or magnetic conductors including semiconductors and metals [6–10]. Although the physical mechanisms of the SHE and ISHE are divided into intrinsic and extrinsic mechanisms [11,12], both mechanisms stem from the relativistic spin-orbit coupling (SOC) that scatters the spin-up and spin-down electrons to opposite transverse directions to achieve the spin-charge interconversion. The efficiency of the spin-charge interconversion is quantified as the spin Hall angle θ_{SH}. Since heavy atoms possess a strong SOC, relatively large θ_{SH} is generally found in heavy metals [13], light metals doped with heavy atoms [14], and compounds with heavy atoms [15]. In particular, θ_{SH} is roughly proportional to Z^4 (Z is the atomic number) for elemental transition metals [16].

Owing to the fact that organic molecules are made of elements with a weak SOC such as hydrogen, carbon, and oxygen, of which the SOC strength is about 1–2 orders of magnitude weaker than that of the Cu atom [17], the SOC strength and the corresponding SHE and ISHE in organic materials are characterized to be rather small. As a result, the SHE or ISHE is expected not to be observable using regular measurement methods. To observe these weak effects, a recent attempt was done by injecting an ultrahigh pure spin current density generated from a permalloy film by the spin pumping effect using a pulsed microwave with power up to a kilowatt, about 4 orders of magnitude larger than the continuous-wave microwave power for the regular spin pumping excitation, into organic materials. A detectable ISHE voltage was thus observed in several different polymers [18]. The ISHE signal or θ_{SH} in the polymers, in which the heavy Pt atoms were intentionally synthesized into the polymer intrachain [19], is much larger than a polymer poly(3,4-ethylenedioxythiophene): poly(4-styrenesulphonate) (PEDOT:PSS), which does not contain any heavy atoms. In contrast, it was found that the polymer PEDOT:PSS exhibited a relatively large ISHE signal where the pure spin current was generated from a 5-μm-thick ferrimagnetic insulator $Y_3Fe_5O_{12}$ (YIG) by the spin pumping effect with less than 40 mW continuous-wave microwave previously [20]. Surprisingly, θ_{SH} of PEDOT:PSS was estimated to be only $\sim 10^{-7}$ in their experiments, in comparison to about 10^{-2} for Pt. The observed extremely small θ_{SH} but relatively large ISHE voltage has been attributed to the large in-plane and out-of-plane conductivity anisotropy that can greatly enhance the spin-charge interconversion efficiency to be comparable to that in Pt [20]. However, the spin lifetime in PEDOT:PSS was estimated to be as long as 5–11 μs. It is difficult to understand the coexistence of a long spin lifetime and high spin-charge interconversion efficiency in the same material [21].

In this work, we carefully investigate the dc voltage signal observed in the PEDOT:PSS/YIG bilayer in spin pumping experiments. We exclude the origin of the observed voltage from the ISHE in PEDOT:PSS by two

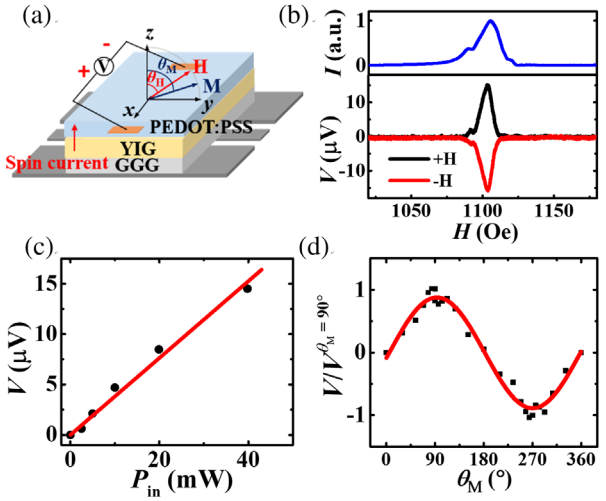

FIG. 1. (a) Sketch of the experimental setup with the pure spin current along the positive z axis. (b) The top panel shows the microwave absorption spectrum of the sample. The bottom panel shows the voltage signal measured in the PEDO:PSS/YIG bilayer as scanning H along the positive (black curve) and negative (red curve) y axis, respectively. The microwave power is 40 mW. (c) The microwave power dependence of the voltage signal and the linear fitting (red curve). (d) θ_M angle dependence of the voltage with $P_{\text{in}} = 40$ mW. The red curve is the $\sin\theta_M$ function fitting.

control experiments: (i) The magnitude of the voltage remains almost unchanged even when the pure spin current is thoroughly blocked by a SiO_2 inserting layer; (ii) the sign of the voltage remains the same when the direction of the pure spin current is reversed by flipping the sample. Interestingly, we found a strong in-plane temperature gradient which has the same angular dependence with the generated voltage. Both vanish when the thickness of the YIG film is reduced to a few nanometers. We thus clarify the physical origin of the observed dc voltage to be the Seebeck effect in the polymer induced by the nonreciprocal magnetostatic surface spin wave (MSSW) propagation in YIG. Our findings can explain the results of the spurious ISHE observed in our spin pumping experiments, as well as those reported by other groups.

The 3.3-μm-thick single-crystalline $Y_3Fe_5O_{12}$ (YIG) film (5×5 mm^2) was grown on a $Gd_3Ga_5O_{12}$ substrate by liquid phase epitaxy. The PEDOT:PSS film was spin-coated onto the YIG film from a water-based solution with 5% in volume dimethyl-sulphoxide (DMSO) to enhance the electrical conductivity and 0.5% surfactant Zonyl-FS300 to improve the wetting properties [22]. The thickness is about 50 nm at a rotation speed of 3000 r/min. Then a pair of copper electrodes were deposited by dc magnetron sputtering with a shadow mask onto the PEDOT:PSS layer, as schematically shown in Fig. 1(a). The sample was then placed on a coplanar waveguide (CPW) in the gap of an electromagnet. A microwave at a frequency $f = 5$ GHz is passed through the CPW. The voltage signal was picked up on two copper electrodes by a Keithley 2182A nanovoltmeter while scanning the external magnetic field. All the experiments were performed at room temperature.

The coordinate system is defined in Fig. 1(a), in which the x axis is along the voltage measurement direction and the z axis is perpendicular to the sample plane. The PEDOT:PSS/YIG bilayer exhibits the microwave absorption at ferromagnetic resonance (FMR) and/or spin wave excitation (SWE) around the resonance field $H_r \sim 1104$ Oe when the magnetic field $\mathbf{H}$ is scanned along the y axis, shown in the top panel in Fig. 1(b). A dc voltage signal V is observed around H_r, as shown by the black curve in Fig. 1(b). When $\mathbf{H}$ is scanned along the opposite direction, V is observed to reverse its sign [red curve in Fig. 1(b)]. The amplitude of V increases linearly with the microwave excitation power P_{in}, as shown in Fig. 1(c). These results were previously explained by the pure spin current $\mathbf{J}_s$ generated by the spin pumping in YIG and then converted to a dc voltage via ISHE in PEDOT:PSS [20].

We further measured V while scanning $\mathbf{H}$ in the yz plane with an angle θ_H between $\mathbf{H}$ and the z axis [Fig. 1(a)]. The results are shown in Fig. 1(d), in which θ_M is the angle between the magnetization $\mathbf{M}$ of YIG and the z axis. $\mathbf{M}$ is noncollinear with $\mathbf{H}$ due to the demagnetization field. Given the weak in-plane anisotropy of YIG, θ_M is calculated by taking into account only the demagnetization field: $2H\sin(\theta_H - \theta_M) + 4\pi M_s \sin 2\theta_M = 0$, where M_S is the saturation magnetization of YIG [23,24]. For the ISHE, the ISHE voltage signal V_{ISHE} is given by $V_{\text{ISHE}} \propto (\mathbf{J}_S \times \boldsymbol{\sigma})_x$, where $(\mathbf{J}_S \times \boldsymbol{\sigma})_x$ denotes the x component of $\mathbf{J}_S \times \boldsymbol{\sigma}$ and $\boldsymbol{\sigma}$ is the spin polarization direction. $\mathbf{J}_s$ is along the z direction, and $\boldsymbol{\sigma}$ is parallel to $\mathbf{M}$ in this experimental geometry, resulting in $V_{\text{ISHE}} \propto \sin\theta_M$. Indeed, the measured voltage signal can be fitted by a simple $\sin\theta_M$ function very well, as shown by the red curve in Fig. 1(d), consistent with the previous study in the PEDOT:PSS/YIG bilayer and the ISHE mechanism [20]. However, there are several artificial effects that could induce a dc voltage in the spin pumping measurements. To confirm the ISHE mechanism, the control experiments must be carefully performed.

First, we grew a 50-nm-thick SiO_2 film by plasma enhanced chemical vapor deposition on the YIG film before spin-coating the PEDOT:PSS film. The relatively thick SiO_2 interlayer can block the injection of $\mathbf{J}_s$ into the PEDO:PSS film [9]. In such a case, the dc voltage signal is expected to disappear if it originates from the ISHE. However, a dc voltage signal V_{SiO_2} is still observed around H_r, and the sign of V_{SiO_2} is reversed when $\mathbf{H}$ changes its direction, as shown in Fig. 2(a). V_{SiO_2} is found to be proportional to P_{in}, as shown in Fig. 2(b). Moreover, we note that the slope of the linear relationship between V_{SiO_2} and P_{in} is almost the same as that of the sample without SiO_2 [see Fig. 1(c)], indicating that the main contribution of the dc voltage signal observed in PEDOT:PSS/YIG does not come from the ISHE. Furthermore, we measured V_{SiO_2}

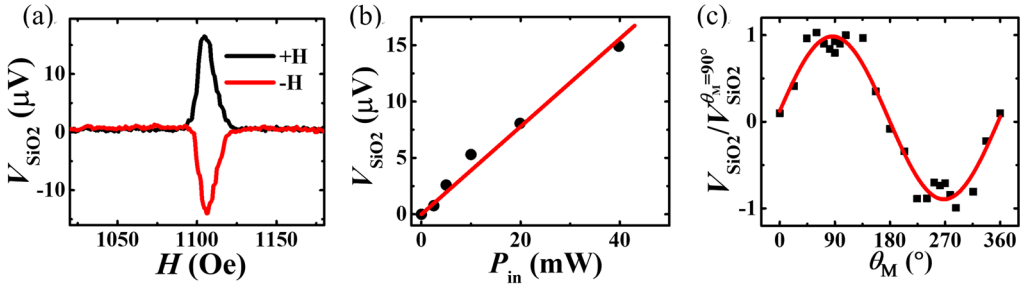

FIG. 2. (a) The voltage signal measured in the PEDO:PSS/YIG bilayer as scanning H along the positive (black curve) and negative (red curve) y axis, respectively. The microwave power is 40 mW. (b) The measured microwave power dependence of the voltage signal and the linear fitting (red curve). (c) θ_M angle dependence of the voltage with $P_{\text{in}} = 40$ mW. The red curve is the $\sin\theta_M$ function fitting.

while $\mathbf{H}$ is scanned in the yz plane, similar to the measurements in Fig. 1(d). Figure 2(c) shows V_{SiO_2} as a function of θ_M. V_{SiO_2} can be fitted by a simple $\sin\theta_M$ function as well. Even though there is no pure spin current in PEDOT:PSS due to the blocking by the relative thick SiO_2 layer, the behaviors are still the same as that of the PEDOT:PSS/YIG bilayer sample. This is strong evidence that the previously used model of the ISHE is not valid to explain the experimental observations in the PEDOT:PSS/YIG bilayer.

To further confirm the nonexistence of the ISHE in PEDOT:PSS, we further performed the second control experiment. According to $V_{\text{ISHE}} \propto (\mathbf{J}_S \times \boldsymbol{\sigma})_x$, V_{ISHE} would change its sign as the sign of $\mathbf{J}_s$ is reversed. $\mathbf{J}_s$ is generated by the spin pumping effect in YIG, meaning that it always transports from YIG to PEDOT:PSS. In the experimental geometry shown in Fig. 1(a), the direction of $\mathbf{J}_s$ is along the positive z axis. The sign of $\mathbf{J}_s$ can be reversed by simply placing the sample upside down [25] and with a polymer solder resist layer being electrically isolated from the CPW, as schematically shown in Fig. 3(a). The results measured in two experimental geometries for the same sample are shown in Fig. 3(b). It is clear that the sign of V remains the same for both experimental geometries. The different amplitudes originate from the different microwave fields acting on the YIG film after its flipping. The observation of

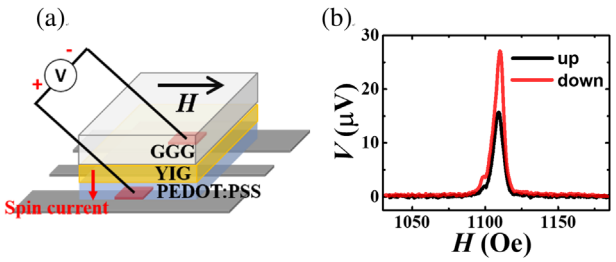

FIG. 3. (a) Sketch of the experimental setup with the pure spin current along the negative z axis. (b) The voltage signal measured in the PEDO:PSS/YIG bilayer as scanning H along the positive y axis for the sample measured in the experimental setup shown in Fig. 1(a) (black curve) and the experimental setup shown in (a) (red curve), respectively.

the dc voltage with the same sign cannot be explained by the ISHE. With these two control experimental results, we can unambiguously conclude that the observed dc voltage is irrelevant to the ISHE in the PEDOT:PSS film.

We attribute the observed dc voltage to the Seebeck effect in PEDOT:PSS with the thermal gradient caused by the unidirectional spin wave propagation on the surfaces of YIG. When the YIG film is put on a CPW or a microstrip line, the microwave field can excite the MSSWs on the top and bottom of the film [26]. The MSSWs propagate in the direction of $\mathbf{M} \times \mathbf{n}$, where $\mathbf{M}$ is the magnetization and $\mathbf{n}$ is the surface normal, meaning that the MSSWs propagate in opposite directions at the two surfaces of YIG, known as a nonreciprocal phenomenon [27,28]. Since the Gilbert damping constant in YIG is extremely low, the MSSWs can convey the energy and then emit heat at a distance up to 10 mm [29,30]. Owing to the inhomogeneous microwave field for a microstrip line in the YIG film thickness direction, the amplitude of the excited MSSWs at the surface close to the microstrip line is larger than that at the other surface. The effect is pronounced when the film is thick. For instance, an in-plane temperature gradient ΔT_x of $\sim$2 K perpendicular to $\mathbf{M}$ can be created in a 4-mm-long YIG with $P_{\text{in}} = 20$ mW [29]. Considering a large Seebeck coefficient $S_{\text{PEDOT:PSS}}$ of PEDOT:PSS [31], a relative large Seebeck voltage could be obtained.

To verify that the nonreciprocal MSSW propagation indeed induces ΔT_x, we measured ΔT_x in the YIG film in the spin pumping experimental setup. We deposited Cu films at the two ends of the YIG film by sputtering through a shadow mask to form two small Hall bars as the thermometers, as schematically shown in Fig. 4(a). The insets in the top and middle panels in Fig. 4(b) show the resistances of the two Cu strips [labeled as $R1$ and $R2$ in Fig. 4(a)], respectively, measured by a four-probe method as a function of the temperature around room temperature. Then the resistance-temperature relations of $R1$ and $R2$, respectively, are utilized to determine the local temperature. The resistances of $R1$ and $R2$ exhibit peaks around resonance with $P_{\text{in}} = 40$ mW as scanning the magnetic field, shown in the top and middle panels in Fig. 4(b), indicating that the YIG film absorbs the microwave energy and is heated up.

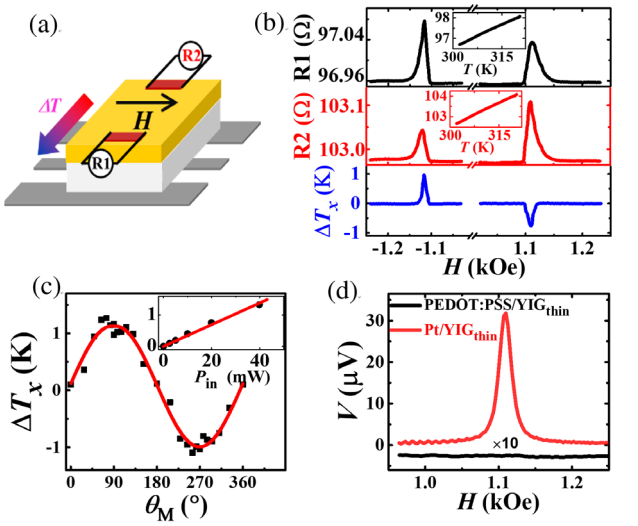

FIG. 4. (a) Experimental setup for the temperature gradient measurement. (b) The resistance as a function of H for $R1$ (top panel) and $R2$ (middle panel). The insets are the resistance of $R1$ (black curve) and $R2$ (red curve) as a function of the temperature, respectively. The bottom panel shows ΔT_x as a function of H. (c) θ_M angle dependence of ΔT_x. The red curve is the $\sin\theta_M$ function fitting. The inset is the microwave power dependence of ΔT_x and the linear fitting (red curve). (d) The voltage signal as a function of H measured in the $\mathrm{Pt/YIG_{thin}}$ and PEDOT:$\mathrm{PSS/YIG_{thin}}$ samples with $P_{\mathrm{in}} = 300$ mW.

The resistance and the corresponding temperature of $R1$ (T_1) at the negative resonance field is higher than those at the positive resonance field. On the contrary, the temperature of $R2$ (T_2) at the negative resonance field is lower than that at the positive resonance field. We plotted $\Delta T_x = T_1 - T_2$ as a function of H in the bottom plane in Fig. 4(b). Obviously, ΔT_x of ~1 K is built-in YIG at the resonance field, and it reverses sign as changing the direction of $\mathbf{M}$. Since the Seebeck coefficient of our PEDOT:PSS films is measured to be 6.4–24.3 μV/K [32], a Seebeck voltage $V_{\mathrm{S}} = S_{\mathrm{PEDOT:PSS}} \times \Delta T_x \sim 10\ \mu$V is estimated in the PEDOT:PSS/YIG bilayer, comparable with the magnitude of the observed voltage [Fig. 1(c)]. The shapes of the ΔT_x curve resemble the voltage signals shown in Figs. 1(b), 2(a), and 3(b). The magnitude of ΔT_x linearly increases with P_{in}, as shown in the inset in Fig. 4(c). We further measured the dependence of ΔT_x on θ_M, similar to the measurements in Fig. 1(d). The results are shown in Fig. 4(c). It is clear that ΔT_x can be well fitted by a $\sin\theta_M$ function [red curve in Fig. 4(c)], identical with the observed dc voltage angular dependence. These results strongly suggest that the observed voltage signal originates from the Seebeck effect in PEDOT:PSS.

It may be argued that the voltage signal should disappear at the FMR field, since FMR arises from a wave vector $\boldsymbol{k} = 0$ spin wave. In fact, $\boldsymbol{k} \neq 0$ spin waves can also be excited under FMR conditions. These spin waves have a MSSW component, leading to a temperature gradient and hence a voltage signal at the FMR field [32,33].

Based on the above measurements on ΔT_x, the behaviors of the observed V measured in the PEDOT:PSS/YIG bilayer and two control experiments can be well understood by the model of the Seebeck effect in PEDOT:PSS. Given that $S_{\mathrm{PEDOT:PSS}}$ is independent on $\mathbf{M}$ of YIG, the behaviors of the Seebeck voltage V_{S} in PEDOT:PSS correlated with $\mathbf{M}$ come only from ΔT_x. Therefore, we get $V_S \propto \Delta T_x \propto P_{\mathrm{in}}$ and $V_S \propto \Delta T_x \propto \sin\theta_M$, consistent with the results shown in Figs. 1(c) and 1(d). In the control sample of PEDOT:PSS/$\mathrm{SiO_2}$/YIG, the heat can easily transfer through the 50-nm-thick $\mathrm{SiO_2}$ film [34], meaning that ΔT_x in YIG is maintained in PEDOT:PSS nearly without reducing the amplitude of ΔT_x. As a result, we observed that the amplitude and the behaviors of the voltage signal measured in PEDOT:PSS/$\mathrm{SiO_2}$/YIG (Fig. 2) are almost the same as those measured in the sample without the $\mathrm{SiO_2}$ layer (Fig. 1). For the second control experiment, the amplitude of the MSSWs at the surface of YIG closer to the CPW is larger than that at the other surface owing to the inhomogeneous microwave field generated by the CPW. It means that the MSSWs at the surface closer to the CPW always transfer more heat than those at the other surface in two experimental geometries [Figs. 1(a) and 3(a)]. Therefore, the sign of ΔT_x and V_S would not change by flipping over the sample. The magnitude of V_S for the sample upside down geometry is larger than that for the sample facing up geometry [Fig. 3(b)]. This is because the YIG film is closer to the CPW in the sample upside down geometry than in the sample facing up geometry, resulting in the microwave magnetic field on YIG and the corresponding ΔT_x in the former geometry larger than that in the latter geometry.

ΔT_x is caused by the nonreciprocal MSSW propagation, meaning that ΔT_x would disappear without the nonreciprocal phenomenon. This could occur in a very thin YIG film [35]. To confirm the validity of our model, we preformed the spin pumping experiment on a YIG film with a thickness of only 10 nm (labeled as $\mathrm{YIG_{thin}}$). For this purpose, we epitaxially grew a thin YIG film by pulsed laser deposition. The growth process and characterization of the YIG film have been described in detail in our previous report [36]. Indeed, the in-plane temperature gradient is not observed in $\mathrm{YIG_{thin}}$ [32]. Furthermore, we prepared a 5-nm Pt film and a 50-nm PEDOT:PSS film on two $\mathrm{YIG_{thin}}$ films, respectively. The Pt/YIG sample is a typical system to exhibit the spin pumping and ISHE. A dc voltage up to 30 μV is detected around the resonance field with $P_{\mathrm{in}} = 300$ mW in $\mathrm{Pt/YIG_{thin}}$, shown in Fig. 4(d), consistent with the previous reports [37]. In sharp contrast, we did not observe the electrical voltage down to 50 nV in the PEDOT:PSS/$\mathrm{YIG_{thin}}$ sample, even though P_{in} is as high as 300 mW, as shown in Fig. 4(d). This result means that the spin-charge interconversion efficiency in PEDOT:PSS is more than 2 orders of magnitude smaller than that in Pt, inconsistent with the previous report [20]. Moreover, this result strongly suggests that the observed voltage signal in the PEDOT:PSS/YIG bilayer is related with the MSSW propagation.

In conclusion, we have systematically investigated the dc voltage generation in the heterostructure of PEDOT:PSS and micrometer-thick YIG under FMR and/or SWE conditions. The voltage signal disappears when an SiO_2 layer is inserted to block the pure spin current. And it does not change its sign when the sample is placed upside down. These results unambiguously exclude the ISHE in PEDOT:PSS. Moreover, a temperature gradient is observed, and it has the same angular dependence with the generated dc voltage. Both the temperature gradient and dc voltage vanish when the thickness of YIG film is reduced to 10 nm. We thus conclude that the dc voltage generation is caused by the Seebeck effect in PEDOT:PSS where the temperature gradient is induced by the nonreciprocal MSSW propagation. In addition, this unidirectional spin-wave-propagation-induced Seebeck voltage could also occur in a heterostructure of micrometer-thick YIG and a material with a large Seebeck efficient such as graphene and topological insulators.

This work was supported by National Key R&D Program of China (2017YFA0303202) and National Natural Science Foundation of China (51471086, 11674159, and 11727808).

*Corresponding author.
djshu@nju.edu.cn
†Corresponding author.
hfding@nju.edu.cn
‡Corresponding author.
dwu@nju.edu.cn

[1] E. Saitoh, M. Ueda, H. Miyajima, and G. Tatara, Appl. Phys. Lett. **88**, 182509 (2006).
[2] Y. K. Kato, R. C. Myers, A. C. Gossard, and D. D. Awschalom, Science **306**, 1910 (2004).
[3] J. Grollier, V. Cros, A. Hamzic, J. M. George, H. Jaffrès, A. Fert, G. Faini, J. Ben Youssef, and H. Legall, Appl. Phys. Lett. **78**, 3663 (2001).
[4] S. O. Valenzuela and M. Tinkham, Nature (London) **442**, 176 (2006).
[5] J. S. Moodera, L. R. Kinder, T. M. Wong, and R. Meservey, Phys. Rev. Lett. **74**, 3273 (1995).
[6] J. Sinova, S. O. Valenzuela, J. Wunderlich, C. H. Back, and T. Jungwirth, Rev. Mod. Phys. **87**, 1213 (2015).
[7] K. Ando and E. Saitoh, Nat. Commun. **3**, 629 (2012).
[8] T. Kimura, Y. Otani, T. Sato, S. Takahashi, and S. Maekawa, Phys. Rev. Lett. **98**, 156601 (2007).
[9] B. F. Miao, S. Y. Huang, D. Qu, and C. L. Chien, Phys. Rev. Lett. **111**, 066602 (2013).
[10] K. Ando, S. Takahashi, J. Ieda, Y. Kajiwara, H. Nakayama, T. Yoshino, K. Harii, Y. Fujikawa, M. Matsuo, S. Maekawa, and E. Saitoh, J. Appl. Phys. **109**, 103913 (2011).
[11] T. Tanaka, H. Kontani, M. Naito, T. Naito, D. S. Hirashima, K. Yamada, and J. Inoue, Phys. Rev. B **77**, 165117 (2008).
[12] M. Gradhand, D. V. Fedorov, P. Zahn, and I. Mertig, Phys. Rev. Lett. **104**, 186403 (2010).
[13] A. Hoffmann, IEEE Trans. Magn. **49**, 5172 (2013).
[14] Y. Niimi, M. Morota, D. H. Wei, C. Deranlot, M. Basletic, A. Hamzic, A. Fert, and Y. Otani, Phys. Rev. Lett. **106**, 126601 (2011).
[15] P. Deorani, J. Son, K. Banerjee, N. Koirala, M. Brahlek, S. Oh, and H. Yang, Phys. Rev. B **90**, 094403 (2014).
[16] H. L. Wang, C. H. Du, Y. Pu, R. Adur, P. C. Hammel, and F. Y. Yang, Phys. Rev. Lett. **112**, 197201 (2014).
[17] Z. G. Yu, Phys. Rev. B **85**, 115201 (2012).
[18] D. Sun, K. J. van Schooten, M. Kavand, H. Malissa, C. Zhang, M. Groesbeck, C. Boehme, and Z. V. Vardeny, Nat. Mater. **15**, 863 (2016).
[19] C.-X. Sheng, S. Singh, A. Gambetta, T. Drori, M. Tong, S. Tretiak, and Z. V. Vardeny, Sci. Rep. **3**, 2653 (2013).
[20] K. Ando, S. Watanabe, S. Mooser, E. Saitoh, and H. Sirringhaus, Nat. Mater. **12**, 622 (2013).
[21] M. P. de Jong, L. J. van IJzendoorn, and M. J. A. de Voigt, Appl. Phys. Lett. **77**, 2255 (2000).
[22] M. Vosgueritchian, D. J. Lipomi, and Z. Bao, Adv. Funct. Mater. **22**, 421 (2012).
[23] V. Castel, N. Vlietstra, J. Ben Youssef, and B. J. van Wees, Appl. Phys. Lett. **101**, 132414 (2012).
[24] S. W. Jiang, S. Liu, P. Wang, Z. Z. Luan, X. D. Tao, H. F. Ding, and D. Wu, Phys. Rev. Lett. **115**, 086601 (2015).
[25] W. Zhang, B. Peng, F. Han, Q. Wang, W. T. Soh, C. K. Ong, and W. Zhang, Appl. Phys. Lett. **108**, 102405 (2016).
[26] J. R. Eshbach and R. W. Damon, Phys. Rev. **118**, 1208 (1960).
[27] K. L. Wong, L. Bi, M. Bao, Q. Wen, J. P. Chatelon, Y.-T. Lin, C. A. Ross, H. Zhang, and K. L. Wang, Appl. Phys. Lett. **105**, 232403 (2014).
[28] T. Schneider, A. A. Serga, T. Neumann, B. Hillebrands, and M. P. Kostylev, Phys. Rev. B **77**, 214411 (2008).
[29] T. An, V. I. Vasyuchka, K. Uchida, A. V Chumak, K. Yamaguchi, K. Harii, J. Ohe, M. B. Jungfleisch, Y. Kajiwara, H. Adachi, B. Hillebrands, S. Maekawa, and E. Saitoh, Nat. Mater. **12**, 549 (2013).
[30] A. A. Serga, A. V. Chumak, and B. Hillebrands, J. Phys. D **43**, 264002 (2010).
[31] B. Zhang, J. Sun, H. E. Katz, F. Fang, and R. L. Opila, ACS Appl. Mater. Interfaces **2**, 3170 (2010).
[32] See Supplemental Material at http://link.aps.org/supplemental/10.1103/PhysRevLett.120.047201 for the Seebeck coefficient measurement of the PEDOT:PSS film, temperature gradient in YIG_{thin} film under FMR and/or SWE, and spin wave propagation under FMR conditions, which includes Ref. [33].
[33] R. E. De Wames and T. Wolfram, J. Appl. Phys. **41**, 987 (1970).
[34] S.-M. Lee and David G. Cahill, J. Appl. Phys. **81**, 2590 (1997).
[35] P. Pirro, T. Brächer, A. V. Chumak, B. Lägel, C. Dubs, O. Surzhenko, P. Görnert, B. Leven, and B. Hillebrands, Appl. Phys. Lett. **104**, 012402 (2014).
[36] P. Wang, S. W. Jiang, Z. Z. Luan, L. F. Zhou, H. F. Ding, Y. Zhou, X. D. Tao, and D. Wu, Appl. Phys. Lett. **109**, 112406 (2016).
[37] O. D'Allivy Kelly, A. Anane, R. Bernard, J. Ben Youssef, C. Hahn, A. H. Molpeceres, C. Carrétéro, E. Jacquet, C. Deranlot, P. Bortolotti, R. Lebourgeois, J. C. Mage, G. De Loubens, O. Klein, V. Cros, and A. Fert, Appl. Phys. Lett. **103**, 082408 (2013).